The Effect of Atmosphere on the Structure and Properties of Selective Laser Melted Al-12Si Alloy

X. J. Wang[a,b], X.P. Li[a], L. C. Zhang[c] , M. H. Fang[b], and T. B. Sercombe[a, *]

[a]*School of Mechanical and Chemical Engineering, The University of Western Australia, 35 Stirling Highway, Crawley, Perth, WA 6009, Australia*

[b]*School of Materials Science and Technology, China University of Geosciences (Beijing), No.* 29 *Xueyuan Road, Haidian District, Beijing 100083, China*

[c]*School of Engineering, Edith Cowan University, 270 Joondalup Drive, Joondalup, Perth, WA 6027, Australia*

Abstract

Al-12Si components were manufactured by Selective Laser Melting (SLM) using three different atmospheres: argon, nitrogen and helium. The atmosphere type did not affect the part's density or hardness and all components reached near full relative density (>97%). The mechanical properties of the components produced in Ar and N_2 were superior to those in He, especially the ductility, which has been attributed to the formation of pore clusters in the microstructure. The mechanical properties in SLM-produced components are superior to those produced using conventional method.

Keywords: Aluminium alloys; selective laser melting; mechanical properties; Atmosphere; microstructure; atmosphere

* Corresponding author. Email: tim.sercombe@uwa.edu.au

Introduction

Aluminium and its alloys are widely used in engineering structures and components because of its light weight and high corrosion resistance. Traditional fabrication methods of aluminium components such as casting, forging, and extrusion require tooling or dies to shape the parts. These are relatively expensive and time-consuming to produce, especially for small production runs of complex parts. Indirect rapid manufacturing of aluminium components is possible, but requires a two-stage process of green part production followed by infiltration [1]. It therefore takes 2-3 days to produce a part. There are other indirect methods but they typically require the production of a lost wax model and subsequent investment casting, which is not a true rapid manufacturing technology as it still requires the fabrication of a mould. More recently, the production of aluminium components directly from a computer model has become possible through a process known as Selective Laser Melting (SLM) [2-9]. During the SLM process, a high intensity laser beam selectively scans a thin powder bed, melting the metal particles which solidify to form a solid layer. The build platform then moves down by the thickness of one layer (typically 50-100μm), a new layer of powder is deposited on top and the process continues until the part is complete. One of the key advantages of SLM is its ability to produce near need for any tooling or machining [1, 10-12]. For the SLM of aluminium, work has concentrated on the processing of an alloy commonly refered to at AlSi10Mg (nominal composition Al – 10 wt% Si - 0.4 wt% Mg) [2, 3, 6-9], which is equivalent to the casting alloy A360.0 [13]. There has been considerably less work published on Al-12Si and 6061[4, 5], both of which reported low densities.

Selective Laser Melting is a complex physical metallurgical process, involving many parameters (typically including scanning speed, laser power, scan spacing, layer thickness, and scanning strategy), and it therefore requires a comprehensive understanding of the effect of these for optimal manufacturing. Considerable effort has been expended on a wide range of materials (including aluminium) to optimize the parameters with the aim of improving density (see, for example, [4, 5, 11, 14, 15]) and surface quality/roughness [8, 11, 16, 17] In addition, the build orientation has been shown to have an effect on the properties of SLM produced parts, with the vertical (build) direction resulting in the lowest properties [6, 18, 19]. Among all the processing parameters, the effect of laser scan speed, laser power, layer thickness has been the most widely studied. In contrast, there has only been a small amount of work focused on the effect of atmospheric oxygen content on the quality of laser melted parts [20]. For the processing of Al-based alloys, the atmosphere used has been either Ar [2, 4-7] or not stated [3, 8, 9]. Hence it is apparent that role of the atmosphere type has not been studied in detail.

During the conventional press-and-sinter processing of metals, the atmosphere is often reactive and used for such purposes as oxide reduction and binder/lubricant removal [21]. For the sintering of aluminium, it is generally considered that a nitrogen atmosphere is more effective for densification than other atmospheres [22, 23]. This has been attributed to the reaction of the Al with the nitrogen to form aluminium nitride [22-25]. However, little has been reported on the role of the atmosphere during Selective Laser Melting. In this work, we have reported that the atmosphere type has essentially no effect on the densification process during selective laser melting but

does have some effect on the mechanical properties of the resultant parts.

Experimental

The details of the Al-12Si powder used in this work are summarized in Table 1. The composition of the powder was measured using inductively coupled plasma atomic emission spectroscopy (Spectrometer Services Victoria, Australia). Flowability and apparent density was measured according to Metal Powder Industries Federation Standards 03 and 04 [26], respectively. Nitrogen content of laser melted parts was measured using Leco nitrogen analysis (Spectrometer Services Victoria, Australia). Three samples from each atmosphere were analysed. The particle size was measured using a Malvern Mastersizer Plus. A scanning electron image (Tescan Vega3) of the powder, Figure 1, shows that it is almost spherical in shape, and contains significant numbers of satellites. Selective laser melting was performed on a Realizer SLM 100 (ReaLizer GmbH, Germany). Prior to building the chamber was purged with either an argon, nitrogen or helium atmosphere until the oxygen content was <0.1%. In all cases, the gases were of high purity, containing <10ppm O_2. During building, a slight positive pressure of 10 to 30 mbar was maintained inside the chamber. Cubes with dimension of 10 × 10 × 10 mm^3 were manufactured using a laser power (at the part bed) of 200 W (λ=1.06μm), laser beam diameter of 35μm, laser scan speeds between 375 – 2000 mm s^{-1}, and hatch spacing (distance between scan lines) of 0.15 mm. Parts were built by scanning the laser across the surface in 3mm stripes. The direction of scanning was rotated through 90º between successive layers. The layer thickness was kept constant at 50 μm. Density was measured using Archimedes' method, following Metal Powder Industries Federation Standard 42

[26], and is presented as a percentage of the theoretical density (2.65g/cm^3). For each condition, three specimens were measured and the results averaged. The microstructure of the XZ (vertical) section was examined by mounting the samples in epoxy and polishing using standard metallographic techniques. Optical microscopy was performed on unetched samples using an Olympus PMG3 optical microscope. The microstructure was also investigated at high magnification using a Zeiss 1555 VP-FESEM. Vickers Hardness was measured on the polished cross-sections using a Mitutoya AVK-C2 Hardness Tester with a 20 g load. An average of twelve indents was taken for each condition. Tensile tests were carried out on as fabricated, but machined specimens, using an Instron 5982 machine at a cross head speed of 1mm/min. The samples had a cross-sectional area of 4 x 6mm and the size of the parallel gauge length was 16mm. The reported tensile properties are the average of five individual samples that had been built aligned to the x-direction (i.e. perpendicular to the build direction), as shown in Figure 2.

Results and Discussion

Figure 3 shows the effect of incident volumetric laser energy density and laser scan speed on the density of the SLM-produced samples under high purity argon, nitrogen and helium atmospheres. The volumetric laser energy density, E, is a key factor that affects the quality of parts fabricated by selective laser melting and is a measure of the energy supplied by the laser beam to a volumetric unit of powder and is defined by [15]

$$E = \frac{P}{v \cdot h \cdot t} \qquad \textit{Equation 1}$$

where P is the laser power (W), v is the scan speed (mm s^{-1}), h is the hatch spacing (mm), and t is the layer thickness (mm). As Equation 1 shows, a lower laser power

and/or higher scan speed, hatch distance or layer thickness decreases the laser energy density, which is needed to heat and melt the powder. From Figure 3, it is apparent that for all atmospheres, the density of the samples increases with increasing E up to ~30 J/mm^3, at which point the samples are >97% dense. Further increasing the energy did not result in any improvement in the density. Hence, it appears that once the powder has become fully molten, there is little benefit in increasing the energy further. In fact, excess energy can be detrimental for the surface finish as it can result in balling [16]. Below this threshold energy level of ~30J/mm^3, there is insufficient energy to completely melt the powder, which results in porosity and a decrease in density [5]. In all three atmospheres, the same trend is evident, and it may be concluded that there is no significant difference in density between using argon, nitrogen or helium atmospheres.

The Vickers hardness at different scan speeds (volume energy densities) is shown in Figure 4. By comparing Figure 3 with Figure 4, it is apparent that there is a strong correlation between Vickers hardness and density. Again, the atmosphere has essentially no effect on the Vickers Hardness and the peak hardness measured was ~115 HV, which is significantly higher than reported values of as-cast Al-12Si (~85HV) [27] and similar is similar to what has been reported from a Selective Laser Melted AlSi10Mg alloy [6, 9].

Figure 5 shows the microstructure of the vertical section (X-Z) of parts produced under argon, nitrogen and helium at a scan speed of 500 mm s^{-1} (>97% density). This Figure shows the microstructure over a range of magnifications. Fig 5(a), (c), (e) and (g) are at a low magnification and show the general structure of the material. In Figure

5(b), (d), and (f) the microstructure is shown at higher magnification, including an insert which is a high resolution SEM image. In these micrographs, the laser tracks created during the SLM processing are clearly visible. These tracks are typical microstructural features in samples manufactured by selective laser melting [2, 3, 7, 9]. The microstructures produced in the three different atmospheres are very similar over the range of magnifications shown. The structure consists of a cellular Al matrix, surrounded by a nano-meter sized Si particle (the light particles in the insert of Fig 5(b), (d) and (f)). It is apparent that the powders have completely melted and resolidified very quickly, resulting in a microstructure similar to that of rapidly solidified Al-12Si ribbons [28]. The fine scale of the microstructure it a possible reason for the improved hardness over conventionally cast material. For the samples processed in Ar and N_2 there is a small amount porosity remaining in the structure (dark dots in Fig 5(a) and (c)). In He however, there seems to be two different microstructure formed (in terms of porosity). The majority of the microstructure is similar to that produced in Ar or N_2, and is shown Fig 5(e). However, in isolated areas, a high porosity region occurs, Fig 5(g), which consists of spherical pores up to approximately 50μm in diameter. It is apparent that the size of these areas is quite low, as the overall density is unaffected. Why such porous regions form is not currently understood, however they have a consequence for the mechanical properties, as discussed below.

The as-processed tensile properties at different energy levels/scan speeds are shown in Figure 6. Similar to the density and hardness, there is an overall trend of increasing strength and ductility with increasing laser energy density for all three

atmospheres. At low laser energies, the high level of porosity degrades the tensile properties of the material, irrespective of the atmosphere used. An increase porosity causing an adverse effect on the properties has been well documented for both casting [29-32] and Selective Laser Melting [12, 33, 34]. However, when processed under the same conditions (which produces parts of the same density – see Figure 3), samples produced in He have reduced ductility and also slightly lower ultimate tensile strength, compared to those samples produced in Ar and N_2. This difference is also shown in Table 2. For these samples, which have all been processed at a laser scan speed of 500mm/s, there is no statistical difference in the density. However, it is evident that the properties, especially the ductility, are significantly lower in He than in Ar or N_2 (which have similar properties). The reason for the lower ductility may be explained with reference to Figure 7. This Figure shows that the sample processed in He contains significantly more porosity on the fracture surface than those produced in Ar or N_2. The properties, particular the ductility, of cast Al-Si alloys have a strong correlation with the amount of porosity present on the facture surface [35, 36]. In particular, it is the projected area of the micro-voids on the fracture surface, rather than the volumetric porosity as measured by the bulk density, that is most important [37, 38]. Since SLM can be considered as repeated micro-scaled casting events, it is not surprising that the same effects appear to be occurring here. Although the overall bulk density is similar in all three atmospheres, there is clustering of pores in the samples produced in He, through which the failure occurs (Figure 7(c)). These clusters, therefore, contribute to the reduced ductility of the samples produced in He.

There is no significant difference in the mechanical properties (Table 3) or nitrogen content (Table 3) of the samples processed in Ar or N_2. During conventional sintering, enhanced densification occurred due to the formation of AlN, which takes some time to form [39]. However, during SLM, the material is only molten for very short time and therefore it is unsurprising that AlN does not form.

Table 2 also compares the mechanical properties of the Al-12Si alloy manufactured by SLM with those of conventionally cast material. The SLM-produced Al-12Si alloy (in an Ar or N_2 atmosphere) has significantly superior properties over the as-cast material. For example, compared with the as-cast properties, the SLM-produced material has approximately 1.5 times the yield strength, 20% greater ultimate tensile strength, and double the elongation to failure. This can be attributed to the morphology of the Si phase, which is present as small, rounded particles in the SLM produced materials compared with the coarse needles typical of castings. Similar improved properties over cast material has been reported in Selective Laser Melted AlSi10Mg [3, 6, 9].

It appears that the role of the atmosphere is only to protect the sample from oxidation and it is not playing an active role in the processes. Due to the fact that there is no difference in processing between Ar and N_2, reduced manufacturing costs may be achieved by using lower cost N_2, rather than the customary Ar.

Conclusion

Samples from an Al-12Si alloy were manufactured by selective laser melting using argon, nitrogen and helium atmospheres. Unlike the conventional sintering of aluminum in which N_2 is the preferred atmosphere, there is no significant difference in density or hardness when using argon, nitrogen or helium. However, results have

shown that a He atmosphere produces lower ductility, probably a result of the formation of pore clusters in the microstructure. Both argon and nitrogen atmospheres result in the SLM produced parts having significantly enhanced properties compared with conventionally produced material: 1.5 times the yield strength, 20% higher ultimate tensile strength and twice the elongation to failure.

Acknowledgements

This research was supported under the Australian Research Council's Discovery Projects funding scheme (DP0986067) and LIEF grant (LE110100094).

References

1. Sercombe, T.B. and G.B. Schaffer, *Rapid Manufacturing of Aluminum Components.* Science, 2003. **301**(5637): p. 1225-1227.
2. Brandl, E., et al., *Additive manufactured AlSi10Mg samples using Selective Laser Melting (SLM): Microstructure, high cycle fatigue, and fracture behavior.* Materials & Design, 2012. **34**(0): p. 159-169.
3. Buchbinder, D., et al., *High Power Selective Laser Melting (HP SLM) of Aluminum Parts.* Physics Procedia, 2011. **12, Part A**(0): p. 271-278.
4. Louvis, E., P. Fox, and C.J. Sutcliffe, *Selective laser melting of aluminium components.* Journal of Materials Processing Technology, 2011. **211**(2): p. 275-284.
5. Olakanmi, E.O., R.F. Cochrane, and K.W. Dalgarno, *Densification mechanism and microstructural evolution in selective laser sintering of Al–12Si powders.* Journal of Materials Processing Technology, 2011. **211**(1): p. 113-121.
6. Kempen, K., et al., *Mechanical Properties of AlSi10Mg Produced by Selective Laser Melting.* Physics Procedia, 2012. **39**(0): p. 439-446.
7. Thijs, L., et al., *Fine-structured aluminium products with controllable texture by selective laser melting of pre-alloyed AlSi10Mg powder.* Acta Materialia, 2013. **61**(5): p. 1809-1819.
8. Calignano, F., et al., *Influence of process parameters on surface roughness of aluminum parts produced by DMLS.* The International Journal of Advanced Manufacturing Technology, 2013. **67**(9-12): p. 2743-2751.
9. Manfredi, D., et al., *From Powders to Dense Metal Parts: Characterization of a Commercial AlSiMg Alloy Processed through Direct Metal Laser Sintering.* Materials, 2013. **6**(3): p. 856-869.
10. Roberts, A.P., et al., *Elastic moduli of sintered powders with application to components fabricated using selective laser melting.* Acta Materialia, 2011. **59**(13): p. 5257-5265.
11. Yasa, E., D. Jan, and K. Jean-Pierre, *The investigation of the influence of laser re-melting on density, surface quality and microstructure of selective laser melting parts.* Rapid Prototyping Journa, 2011. **17**(5): p. 312-327.
12. Zhang, L.C., et al., *Manufacture by selective laser melting and mechanical behavior of a biomedical Ti-24Nb-4Zr-8Sn alloy.* Scripta Materialia, 2011. **65**(1): p. 21-24.
13. *ASM handbook Vol 15 - Casting*. 1990, Materials Park, Ohio: ASM International.
14. Li, R., et al., *Densification behavior of gas and water atomized 316L stainless steel powder during selective laser melting.* Applied Surface Science, 2010. **256**(13): p. 4350-4356.
15. Simchi, A., *Direct laser sintering of metal powders: Mechanism, kinetics and microstructural features.* Materials Science and Engineering: A, 2006. **428**(1–2): p. 148-158.
16. Gu, D. and Y. Shen, *Balling phenomena in direct laser sintering of stainless steel powder: Metallurgical mechanisms and control methods.* Materials & Design, 2009. **30**(8): p. 2903-2910.
17. Spierings, A.B., N. Herres, and G. Levy, *Influence of the particle size distribution on surface quality and mechanical properties in AM steel parts.* Rapid Prototyping Journal, 2011. **17**(3): p. 195-202.
18. Chlebus, E., et al., *Microstructure and mechanical behaviour of Ti—6Al—7Nb alloy produced by selective laser melting.* Materials Characterization, 2011. **62**(5): p. 488-495.
19. Takaichi, A., et al., *Microstructures and mechanical properties of Co–29Cr–6Mo alloy*

fabricated by selective laser melting process for dental applications. Journal of the Mechanical Behavior of Biomedical Materials, 2013. **21**(0): p. 67-76.

20. Rombouts, M., et al., *Fundamentals of Selective Laser Melting of alloyed steel powders.* CIRP Annals - Manufacturing Technology, 2006. **55**(1): p. 187-192.
21. German, R.M., *Powder metallurgy and Particualte Materials Processing*. 2005, Princeton, N.J.: Metal Powder Industries Federation.
22. Schaffer, G.B. and B.J. Hall, *The influence of the atmosphere on the sintering of aluminum.* Metallurgical and Materials Transactions A, 2002. **33**(10): p. 3279-3284.
23. Schaffer, G.B., et al., *The effect of the atmosphere and the role of pore filling on the sintering of aluminium.* Acta Materialia, 2006. **54**(1): p. 131-138.
24. Kent, D., et al., *A novel method for the production of aluminium nitride.* Scripta Materialia, 2006. **54**(12): p. 2125-2129.
25. MacAskill, I.A., et al., *Effects of magnesium, tin and nitrogen on the sintering response of aluminum powder.* Journal of Materials Processing Technology, 2010. **210**(15): p. 2252-2260.
26. *Standard Test Methods for Metal Powders and Powder Metallurgy Products*. 2009, Princeton, New Jersey USA: Metal Powder Industries Federation
27. Basavakumar, K.G., P.G. Mukunda, and M. Chakraborty, *Dry sliding wear behaviour of Al–12Si and Al–12Si–3Cu cast alloys.* Materials & Design, 2009. **30**(4): p. 1258-1267.
28. Birol, Y., *Microstructural evolution during annealing of a rapidly solidified Al–12Si alloy.* Journal of Alloys and Compounds, 2007. **439**(1–2): p. 81-86.
29. Rice, R.W., *Comparison of stress concentration versus minimum solid area based mechanical property-porosity relations.* Journal Of Materials Science, 1993. **28**(8): p. 2187-2190.
30. Roy, N., A.M. Samuel, and F.H. Samuel, *Porosity formation in Al-9 Wt Pct Si-3 Wt Pct Cu alloy systems: Metallographic observations.* Metallurgical and Materials Transactions A, 1996. **27**(2): p. 415-429.
31. Samuel, A.M. and F.H. Samuel, *A metallographic study of porosity and fracture behavior in relation to the tensile properties in 319.2 end chill castings.* Metallurgical and Materials Transactions A, 1995. **26**(9): p. 2359-2372.
32. Sun, X., K.S. Choi, and D.S. Li, *Predicting the influence of pore characteristics on ductility of thin-walled high pressure die casting magnesium.* Materials Science and Engineering: A, 2013. **572**(0): p. 45-55.
33. Kruth, J.P., et al., *Selective laser melting of iron-based powder.* Journal of Materials Processing Technology, 2004. **149**(1-3): p. 616-622.
34. Li, R., et al., *316L Stainless Steel with Gradient Porosity Fabricated by Selective Laser Melting.* Journal of Materials Engineering and Performance, 2010. **19**(5): p. 666-671.
35. Gokhale, A.M. and G.R. Patel, *Origins of variability in the fracture-related mechanical properties of a tilt-pour-permanent-mold cast Al-alloy.* Scripta Materialia, 2005. **52**(3): p. 237-241.
36. Surappa, M.K., E. Blank, and J.C. Jaquet, *Effect of macro-porosity on the strength and ductility of cast Al 7Si 0.3Mg alloy.* Scripta Metallurgica, 1986. **20**(9): p. 1281-1286.
37. Lee, C.D., *Effects of microporosity on tensile properties of A356 aluminum alloy.* Materials Science and Engineering: A, 2007. **464**(1–2): p. 249-254.
38. Lee, C.D., *Variability in the tensile properties of squeeze-cast Al–Si–Cu–Mg alloy.* Materials Science and Engineering: A, 2008. **488**(1–2): p. 296-302.
39. Sercombe, T.B. and G.B. Schaffer, *On the role of magnesium and nitrogen in the infiltration of aluminium by aluminium for rapid prototyping applications.* Acta Materialia, 2004. **52**(10): p.

3019-3025.

40. Suárez-Peña, B. and J. Asensio-Lozano, *Microstructure and mechanical property developments in Al–12Si gravity die castings after Ti and/or Sr additions.* Materials Characterization, 2006. **57**(4–5): p. 218-226.

Table 1. Summary of the characteristics of the Al-12Si powder

Composition (wt %)				Particle size (μm)			Flowability (s/50g)	Apparent density (%)
Al	Si	Fe	Cu	d_{10}	d_{50}	d_{90}	21.0	55.8
Bal	12.2	0.12	0.003	27	38	51		

Table 2. Comparison of the tensile properties for the Al-12Si alloys produced using selective laser melting under purity argon, nitrogen and helium (laser power: 200 W; laser scan speed: 500 mm/s) and by conventional casting method: yield strength $\sigma_{0.2}$, ultimate tensile strength σ_{UTS} and ductility δ. Error bars show one standard deviation. The load was applied perpendicular to the build direction (see Figure 2).

Processing methods	Density (%)	$\sigma_{0.2}$ (MPa)	σ_{UTS} (MPa)	δ (%)	Reference
SLM under N_2	97.8±0.4	224±7	368±11	4.8±0.6	This work
SLM under Ar	97.5±0.3	223±11	355±8	4.2±0.6	This work
SLM under He	97.1±0.4	221±11	342±43	1.5±0.4	This work
Die casting	-	145	300	2.5	[40]

Table 3. Nitrogen content of the powder and SLM'ed parts produced at an energy density of 53 J/mm^3 (at the laser speed of 500 mm/sNo significant difference in the nitrogen content was measured. Three samples were analysed for each condition and the error in the measurement as ±0.01 wt%.

Processing methods	Nitrogen content (wt%)
Powder	<0.01
SLM under N_2	0.01
SLM under Ar	<0.01
SLM under He	0.02

Figure Captions

Figure 1**.** Scanning electron micrograph of the Al-12Si powder used.

Figure 2. Orientation of the tensile bar relative to the building direction.

Figure 3**.** Relative density of the SLM-produced Al-12Si samples as a function of incident laser energy. There is a general trend of increasing density with laser energy density, up to ~30J/mm^3, after which the density plateaus. There is no significant difference between the three atmospheres. Individual points are an average of 3 tests and error bars show one standard deviation.

Figure 4. The effect of laser energy density on the hardness of SLM-produced Al-12Si in Ar, N_2 and He atmospheres. Similar to Fig. 2, the hardness increases with energy density and there is no significant difference between atmospheres. Individual points are an average of 12 tests. Error bars show one standard deviation.

Figure 5. Optical microstructures of the parts manufactured under argon (a) and (b), nitrogen (c) and (d) and helium (f-g) and an energy density of 53 J/mm^3 (500mm/s). With the exception of some areas containing high levels of porosity (g), there is no difference between the microstructures.

Figure 6**.** Tensile properties of the SLM-produced Al-12Si samples under argon, nitrogen and helium. ($\sigma_{0.2}$: yield strength, σ_{UTS}: ultimate tensile strength). There is no difference between the properties of the Ar and N_2 produced samples. For those manufactured in He, the ductility and ultimate tensile strength are significantly reduced.

Figure 7. Fracture surfaces of the Al-12Si samples produced using different

atmosphere (nitrogen, argon and helium). It is apparent that under He, there is significantly more porosity of the fracture surface than in the other two atmospheres.

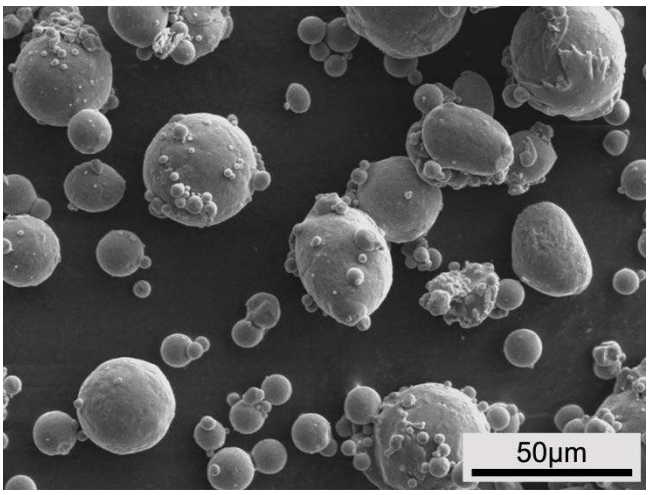

Fig. 1. X.J. Wang et al.

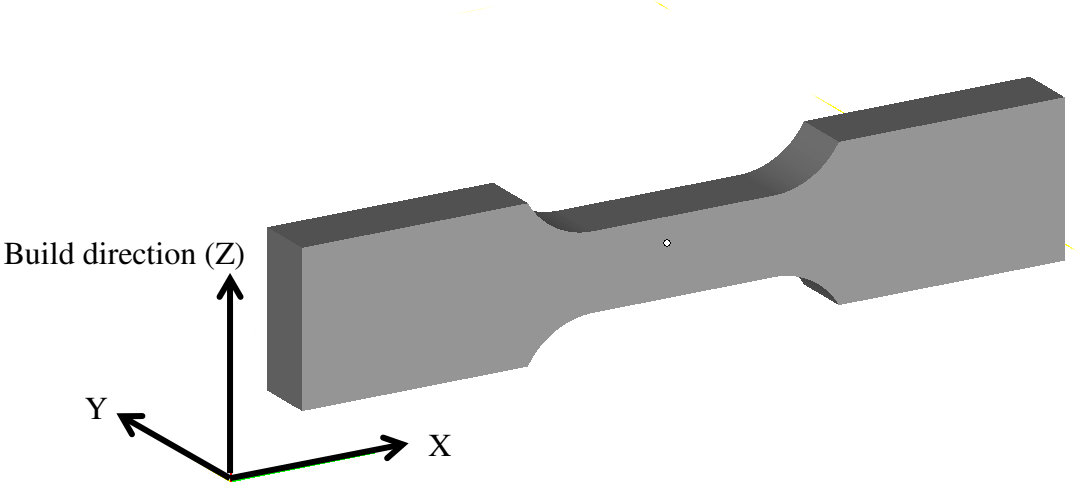

Fig. 2. X.J. Wang *et al*

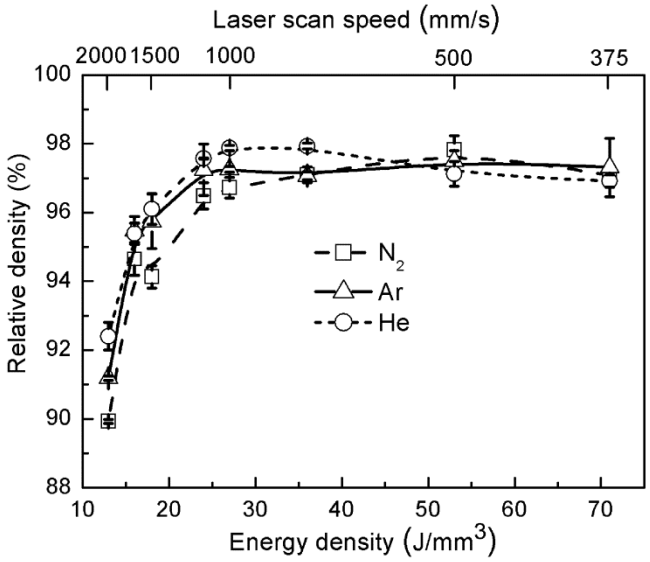

Fig. 3. X.J. Wang *et al.*

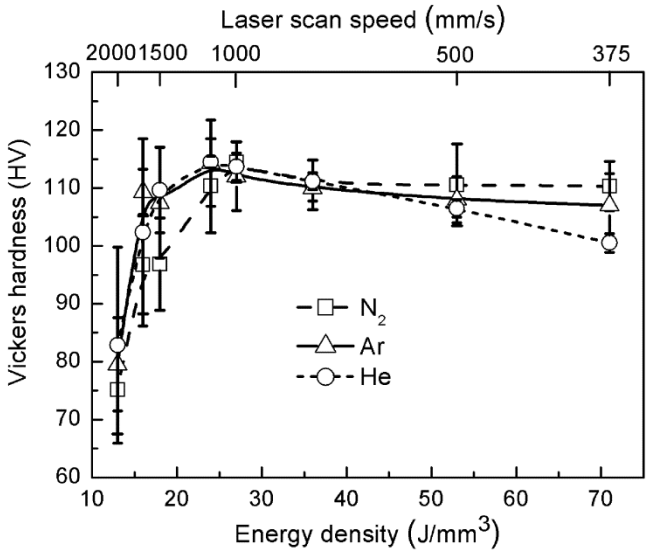

Fig. 4. X.J. Wang *et al.*

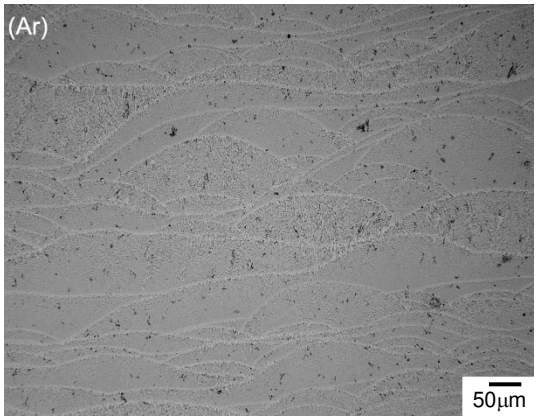
(Ar)
50μm

(a)

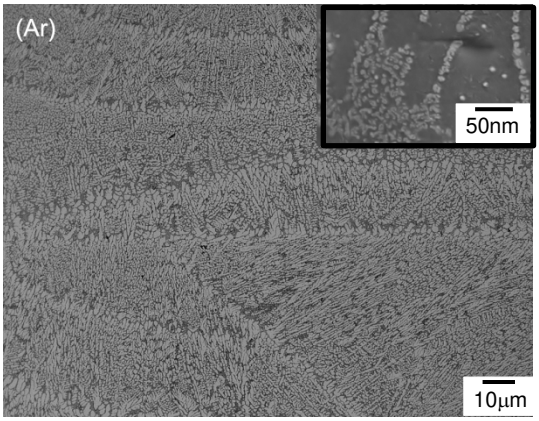
(Ar)
50nm
10μm

(b)

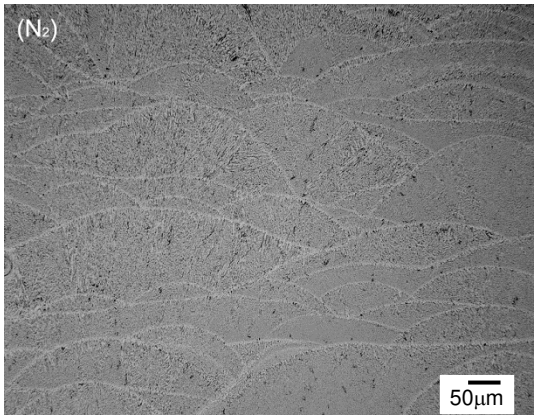
(N2)
50μm

(c)

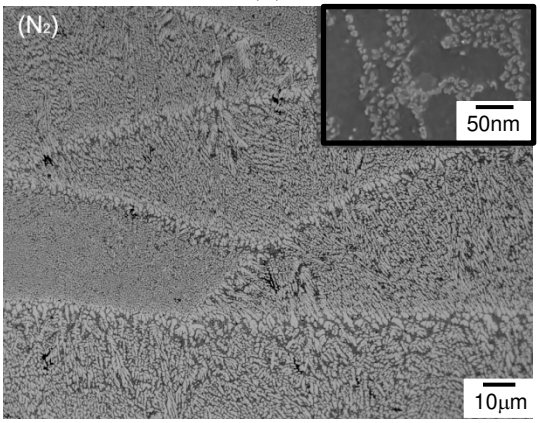
(N2)
50nm
10μm

(d)

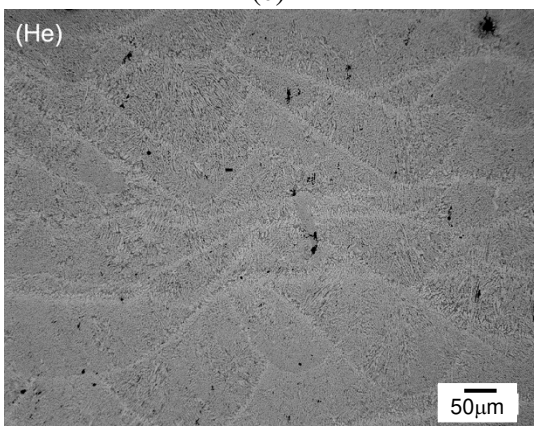
(He)
50μm

(e)

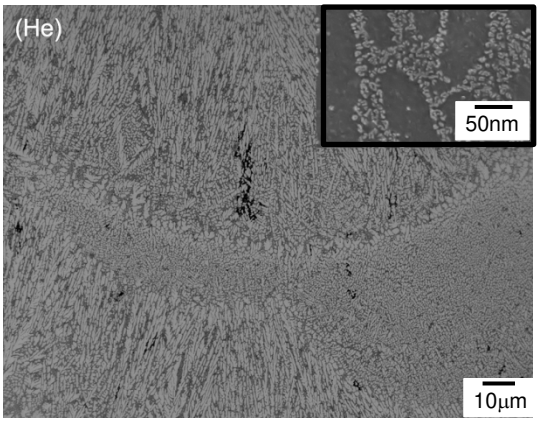
(He)
50nm
10μm

(f)

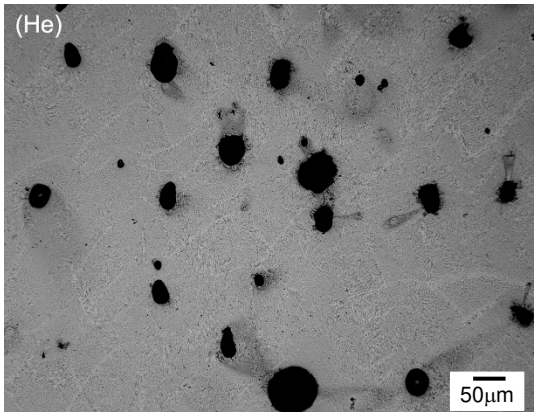
(He)
50μm

(g)

Fig. 5. X.J. Wang *et al.*

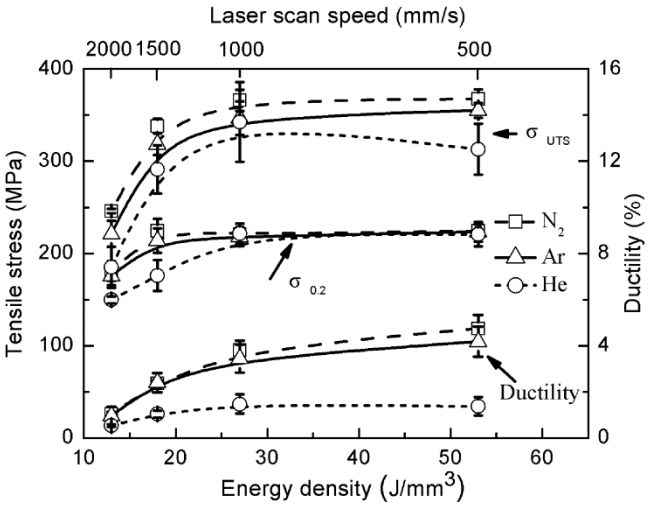

Fig. 6. X.J. Wang *et al.*

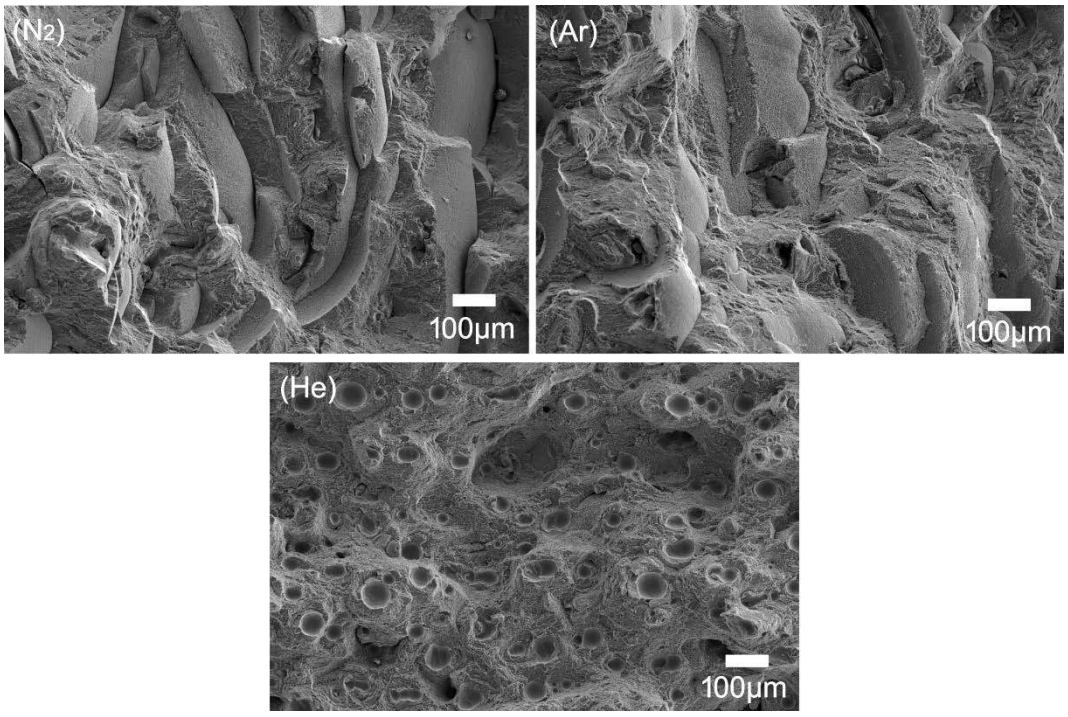

Fig. 7. X.J. Wang *et al.*